Development of 6E3 antibody-mediated SERS immunoassay for drug-resistant influenza virus

Hyeran Kim [a,1], Hyunju Kang [a,1], Hye-Nan Kim [a], Hongki Kim [a], Jeong Moon [a,b], Kyeonghye Guk [a], Hwangseo Park [c], Dongeun Yong [d], Pan Kee Bae [e], Hyun Gyu Park [b], Eun-Kyung Lim [a,f,*], Taejoon Kang [a,**], Juyeon Jung [a,f,***]

[a] Bionanotechnology Research Center, Korea Research Institute of Bioscience and Biotechnology (KRIBB), 125 Gwahak-ro, Yuseong-gu, Daejeon, 34141, Republic of Korea
[b] Department of Chemical and Biomolecular Engineering (BK 21+ Program), Korea Advanced Institute of Science and Technology (KAIST), 291 Daehak-ro, Yuseong-gu, Daejeon, 34141, Republic of Korea
[c] Department of Bioscience and Biotechnology, Sejong University, 209 Neungdong-ro, Kwangjin-gu, Seoul, 05006, Republic of Korea
[d] Department of Laboratory Medicine and Research Institute of Bacterial Resistance, Yonsei University College of Medicine, 50-1 Yonsei-ro, Seodaemun-gu, Seoul, 03722, Republic of Korea
[e] BioNano Health Guard Research Center, 125 Gwahak-ro, Yuseong-gu, Daejeon, 34141, Republic of Korea
[f] Department of Nanobiotechnology, KRIBB School of Biotechnology, University of Science and Technology (UST), 217 Gajeong-ro, Yuseong-gu, Daejeon, 34113, Republic of Korea

ARTICLE INFO

ABSTRACT

Influenza viruses are responsible for several pandemics and seasonal epidemics and pose a major public health threat. Even after a major outbreak, the emergence of drug-resistant influenza viruses can pose disease control problems. Here we report a novel 6E3 monoclonal antibody capable of recognizing and binding to the H275Y neuraminidase (NA) mutation, which has been associated with reduced susceptibility of influenza viruses to NA inhibitors. The 6E3 antibody had a K_D of 72.74 μM for wild-type NA and 32.76 pM for H275Y NA, suggesting that it can identify drug-resistant pandemic H1N1 (pH1N1) influenza virus. Molecular modeling studies also suggest the high-affinity binding of this antibody to pH1N1 H275Y NA. This antibody was also subject to dot-blot, enzyme-linked immunosorbent assay, bare-eye detection, and lateral flow assay to demonstrate its specificity to drug-resistant pH1N1. Furthermore, it was immobilized on Au nanoplate and nanoparticles, enabling surface-enhanced Raman scattering (SERS)-based detection of the H275Y mutant pH1N1. Using 6E3 antibody-mediated SERS immunoassay, the drug-resistant influenza virus can be detected at a low concentration of 10^2 plaque-forming units/mL. We also detected pH1N1 in human nasopharyngeal aspirate samples, suggesting that the 6E3-mediated SERS assay has the potential for diagnostic application. We anticipate that this newly developed antibody and SERS-based immunoassay will contribute to the diagnosis of drug-resistant influenza viruses and improve treatment strategies for influenza patients.

1. Introduction

Pandemics due to viruses are great threats to public health and incur catastrophic effects on the global economy (A. H. Reid et al., 2004; Bedford et al., 2015; Petrova and Russell, 2018; Taubenberger et al., 2019). The United Nations has reported that the current pandemic caused by the severe acute respiratory syndrome coronavirus 2 (SARS-CoV-2) is a global health crisis due to its impact on both health and the

* Corresponding author. Bionanotechnology Research Center, Korea Research Institute of Bioscience and Biotechnology (KRIBB), 125 Gwahak-ro, Yuseong-gu, Daejeon, 34141, Republic of Korea.
** Corresponding author.
*** Corresponding author. Department of Nanobiotechnology, KRIBB School of Biotechnology, University of Science and Technology (UST), 217 Gajeong-ro, Yuseong-gu, Daejeon, 34113, Republic of Korea.
E-mail addresses: eklim1112@kribb.re.kr (E.-K. Lim), kangtaejoon@kribb.re.kr (T. Kang), jjung@kribb.re.kr (J. Jung).
[1] These authors contributed equally to this study.

economy (Sharma et al., 2020). Before the SARS-CoV-2 outbreak, the last pandemic was caused by the influenza H1N1 (pH1N1) virus in 2009 (Medina and García-Sastre, 2011). Approximately 60.8 million cases, 274,304 hospitalizations, and 12,468 deaths were reported in the United States from April 12, 2009, to April 10, 2010, due to pH1N1(Medina and García-Sastre, 2011; Vijaykrishna et al., 2010). Fortunately, pH1N1 is susceptible to the neuraminidase (NA) inhibitors such as oseltamivir, peramivir, and zanamivir, allowing the treatment of influenza virus-infected patients (Hayden et al., 1997; Moscona, 2005; Shetty and Peek, 2012). However, pH1N1 has become one of the causative agents for seasonal influenza, thus remaining a threat to human health. Furthermore, influenza virus isolates that have acquired resistance to NA inhibitors have been reported (Hayden and de Jong, 2011; McKimm-Breschkin, 2013). Therefore, influenza viruses, particularly drug-resistant pH1N1, are poised for re-emergence and may cause large outbreaks in the future. A crucial step in controlling the outbreak of infectious disease is the rapid and accurate detection of virus strains.

Since oseltamivir is the most widely used anti-influenza medication (Moscona, 2005), the re-emergence of oseltamivir-resistant influenza viruses pose a serious threat to human health (Hayden and de Jong, 2011). Oseltamivir resistance of the pH1N1 strain has been reported to be almost always associated with the H275Y mutation, an amino acid substitution from histidine to tyrosine at position 275 of NA (Brookes et al., 2011; Ginting et al., 2012). Since the H275Y mutation is located at the NA active site, the mutation causes damage to the NA structure and consequently interferes with the rearrangement essential for effective oseltamivir binding (Brookes et al., 2011; Tolentino-Lopez et al., 2013). Several studies suggest that the pH1N1 virus carrying the H275Y mutation is gradually becoming dominant, resulting in an increasing number of pH1N1 cases where a prescription for oseltamivir is ineffective (Hurt, 2014; Jones et al., 2019; Meijer et al., 2009). Therefore, it is important to accurately distinguish the H275Y mutant pH1N1 virus from the wild-type (WT) pH1N1.

Influenza virus-infected patients are mainly diagnosed using rapid influenza diagnostic tests (RIDTs), which are immunoassays that can identify the presence of influenza nucleoprotein antigens in respiratory specimens (Green, 2018; Trombetta et al., 2018). Although the methods are rapid, simple, and cost-effective, no commercially available RIDT can distinguish antiviral drug-resistant influenza viruses (Green, 2018). Molecular diagnostic methods can provide information about the antiviral resistance of influenza viruses; however, they are time-consuming, labor-intensive, expensive, and require highly trained personnel and validation of reagents (Jang et al., 2020). The development of immunoassays for drug-resistant influenza viruses will help accurately diagnose drug resistance in patients infected with the influenza virus to guide treatment and prevent further spread of mutant viruses.

Here we report a newly developed 6E3 antibody that specifically recognizes the oseltamivir-resistant influenza virus that carries the H275Y NA mutation. The binding affinity of the 6E3 antibody was verified by enzyme-linked immunosorbent assay (ELISA) and docking simulations. Then, the antibody was applied to different diagnostic formats such as the dot-blot, bare-eye detection using Au nanoparticles (NPs), and lateral flow assay to evaluate its applicability for detecting the H275Y mutant NA. Furthermore, to increase the sensitivity of the system, we immobilized the antibody onto an atomically flat Au nanoplate and Au NPs, acting as an immune substrate and immunoprobe, respectively, and performed surface-enhanced Raman scattering (SERS)-based immunoassay for oseltamivir-resistant pH1N1. SERS is a well-known phenomenon that increases the Raman signals of molecules adjacent to metallic nanostructures (Sharma et al., 2012). SERS-based immunoassay is considered a promising method for viral detection because of its single-molecule sensitivity, molecular fingerprint spectrum, and photostability (Eom et al., 2019a,b; Lee et al., 2018; Sharma et al., 2012). The 6E3 antibody-mediated SERS immunoassay enables us to detect the H275Y mutant influenza virus sensitively and selectively. Moreover, the 6E3-mediated SERS assay allows the diagnosis of the

mutant virus in human nasopharyngeal aspirate samples. Our findings suggest that SERS-based immunoassay using the 6E3 antibody could help diagnose drug-resistant pH1N1 infections and help clinical practitioners to develop an effective treatment for influenza virus infection.

2. Materials and methods

2.1. Materials

All chemicals were purchased from Sigma-Aldrich (MO, USA) unless otherwise specified. Absorbent pads (CFSP203000, cellulose fiber) and NC membrane (HF090MC100) were purchased from Millipore (MA, USA). The polyester conjugate pad was purchased from Boreda Biotech (Seongnam, South Korea). The anti-influenza A virus nucleoprotein antibody (ab20343) was purchased from Abcam (Cambridge, UK). WT and H275Y NA proteins were purchased from Sino Biological (Beijing, China). DENV1-EP, HG-NS1-3-6H, CHIKV-EP2, and JEV-E domain III were provided by the BioNano Health Guard Research Center of South Korea. Cys3-protein G was purchased from Bioprogen (Daejeon, Korea). Malachite green isothiocyanate (MGITC) was purchased from Setareh Biotech (OR, USA). pH1N1 (A/California/07/2009) and H275Y pH1N1 mutant virus (H275Y mutation; A/Korea 2785/2009 pdm: NCCP 42017) were obtained from the National Culture Collection for Pathogens (NCCP) operated by the Korea National Institute of Health (KNH). RSV was obtained from ATCC. The I223 R/H275Y and I223R pH1N1 mutant virus was prepared as previously described (Guk et al., 2020). I223R mutation was introduced within the NA fragment by the forward primer: 5′ AGTTGGAGAAACAATCGTTTGAGAACACAA and reverse primer: 5′ TTGTGTTCTCAAACGATTGTTTCTCCAACT. The titers of viruses were determined using a one-step real-time polymerase chain reaction (RT-PCR) kit (Promega, WI, USA) following the manufacturer's instructions.

2.2. Production of 6E3 antibody

The 6E3 antibody screening procedures are similar to the previous report (Guk et al., 2020). A large naïve human Fab phage display library (3×10^{10}) from the Korea Research Institute of Bioscience and Biotechnology (KRIBB) was used (Guk et al., 2020; Kim et al., 2017). Briefly, immunotubes (Nunc, MA, USA) were coated with 100 μg WT NA or H275Y NA overnight at 4 °C, washed twice with phosphate-buffered saline (PBS), and blocked with skim milk in PBS (4%) for 1 h at 37 °C. The antibody library phages were preincubated with WT NA for 2 h at 37 °C. The subtracted phages were then incubated with H275Y NA for 1 h at 37 °C. After washing with 0.05% Tween 20 in PBS (PBST), bound phages were eluted with glycine-HCl (0.1 M, pH 2.2) and neutralized with Tris base (2 M). The eluted phages were amplified by infecting *Escherichia coli* TG1 cells, followed by superinfection with helper phages (VCSM13) (Marks et al., 1991). The amplified phages were then subject to another round of panning; three rounds of panning were conducted.

After the third round of panning, 500 colonies were randomly selected from the output plate to screen individual clones for specific binding to H275Y NA. The colonies were cultured in Super Broth medium containing ampicillin (100 μg/mL) until an optical density of 0.5 was reached. Fab expression in *E. coli* TG1 cells was induced overnight at 30 °C by adding isopropyl β-D-1-thiogalactopyranoside to a final concentration of 1 mM. The culture supernatant of each clone was subjected to ELISA. In detail, a microtiter plate was coated with 100 ng/well of H275Y NA in sodium carbonate buffer (50 mM, pH 9.6) and incubated at 4 °C overnight. After blocking with 2% BSA in PBS, goat F (ab')2 anti-human IgG (Fab')2-horseradish peroxidase (HRP) antibody (ab98533, Abcam) was used for colorimetric detection of bound clones using the 3,3′,5,5′-tetramethylbenzidine (TMB) substrate (BD Biosciences, CA, USA). Clones showing positive signals in ELISA were subjected to DNA sequencing, and the nucleotide sequences of the variable heavy chain (VH) and variable kappa light chain (VK) regions were determined.

To convert the selected Fabs into the whole IgG format, the VH and VK sequences were amplified by PCR and combined with the leader sequences of IgG heavy and light chains, respectively, by overlap extension PCR using Pfu DNA Polymerase (Thermo Fisher Scientific, MA, USA). The VH and VK with leader sequences were sequentially cloned into the *Eco*RI-*Apa*I and *Hin*dIII-*Bsi*WI sites, respectively, in the antibody expression cassette (pdCMVdhfrC) containing the human constant region of γ1 heavy chain (Cγ1) and Cκ gene (Yoon et al., 2006). For transient IgG expression, the resulting expression plasmid was introduced into HEK293T cells using Lipofectamine (Invitrogen, CA, USA) according to the manufacturer's instructions, and the transfected cells were cultured in protein-free medium (CD293, Invitrogen). IgG was purified from the culture supernatant by affinity chromatography on a protein A-agarose column (Millipore), and its expression and purity were analyzed by western blotting and SDS-PAGE, respectively.

2.3. ELISA

Microtiter wells were coated with the purified WT NA or H275Y NA (100 ng/well) in 50 mM sodium carbonate buffer (pH 9.6) at 4 °C overnight, blocked with BSA (2%) in PBS, and washed with PBST. A purified 6E3 antibody was then added to each well pre-coated with 100 ng NA. HRP-conjugated goat anti-human IgG was used for the detection of bound antibody. Color was developed using the TMB substrate reagent set, and the absorbance at 450 nm was measured using a microtiter plate reader (Emax; Molecular Devices, CA, USA). Affinity was determined as the antigen concentration required to inhibit 50% of binding activity, and the binding affinity (K_D) value was calculated from a Klotz plot. Proteins (100 ng/well; BSA, DENV1-EP, HG-NS1-3-6H, CHIKV-EP2, and JEV-E domain III) and viruses (10^6 PFU/mL; WT pH1N1, H275Y pH1N1, I223R pH1N1, I223 R/H275Y pH1N1, and RSV) were tested using the same procedures.

2.4. Homology modeling of 6E3 antibody

The 3D structure of the 6E3 antibody was constructed by homology modeling using the latest version of the MODELLER program (Šali and Blundell, 1993). As the structural template for the 6E3 antibody, we used the X-ray crystal structure of the Fab fragment of a phage-derived antibody (PDB entry: 2QQN) that specifically blocks the binding of vascular endothelial growth factor (VEGF) to neuropilins (Yu et al., 2012). A high-quality structure was expected in homology modeling because the amino-acid sequences of the 6E3 and the template were 88% identical. The conjugate gradient method and molecular dynamics simulations were applied during the entire course of homology modeling to find the optimal 6E3 structures by minimizing the violation of spatial restraints. The atomic coordinates of the gap regions were calculated from a randomized distorted structure to link the two anchoring atoms, as implemented in the original MODELLER program. The loop regions were modeled with the enumeration algorithm to cope with the structural flexibility (Fiser et al., 2000). Lastly, the calculated structure with the lowest MODELLER objective function was selected as the all-atom model for the 6E3 antibody.

The homology-modeled structure of the 6E3 antibody served as the receptor model to address the differential binding modes between the WT and H275Y mutant NAs. Two pentapeptide fragments comprising residues at the 273–277 position of NA were selected as the simplified models for the WT and H275Y mutant under the assumption that the epitope would include residue 275. Docking simulations of these model epitopes were then performed with the CDR of 6E3 using the AutoDock program to calculate the binding free energies and the optimal binding modes (Morris et al., 1998). Of the 20 binding conformations of the model epitopes generated with the genetic algorithm, those differing by < 1.5 Å in the positional root-mean-square deviation were clustered together. The epitope conformations with the lowest docking free energy in the top-ranked cluster were adopted as the final binding modes

for the 6E3 antibody.

2.5. H275Y pH1N1 detection

For dot-blot analysis, the NC membrane was spotted with WT pH1N1 and H275Y pH1N1 in a two-fold dilution series from 0.92 to 7.4×10^6 PFU/mL. The virus-spotted membrane was incubated with 1 μg/mL of 6E3 in PBS containing 0.1% BSA and 0.05% Tween 20 for 1 h at 25 °C, and then washed three times with PBS containing 0.05% Tween 20. HRP-conjugated goat anti-human IgG was used for the detection of bound IgG. The membrane was covered with the SuperSignal West Femto reagent (Thermo), and chemiluminescence detection was performed with the ChemiDoc system (Bio-Rad, CA, USA).

For colorimetric detection, 10 μg 6E3 antibody was added to a mixture of 1 mL Au NPs (20 nm) and 0.1 mL borate buffer (0.1 M, pH 8.5). After incubation for 30 min at 25 °C, 0.1 mL 1% BSA was added to block the surface of the Au NPs. After incubation for 1 h at 4 °C, the 6E3-Au NPs were collected by centrifugation at $16,000 \times g$ for 15 min at 4 °C and resuspended in deionized water. For the detection of the H275Y pH1N1 virus, a 100 μL virus sample (10^5 PFU/mL) was mixed with 50 μL 6E3-Au NPs and incubated for 30 min. The blank, WT pH1N1 (10^5 PFU/mL), and RSV (10^5 PFU/mL) samples were tested following the same procedure. The absorbance of 6E3-Au NPs was measured using a multidetection microplate reader (Cytation 5, BioTek, VT, USA).

The LFA test strip was prepared as follows. The sample pad was saturated with PBS solution containing 0.2% Tween 20 and 1% BSA. After drying the sample pad at 25 °C, it was stored in a desiccator for future use. The anti-influenza A nucleoprotein IgG-Au NPs were prepared following the procedure for the 6E3-Au NPs but employing the IgG instead of 6E3. The prepared Au NP probes were added to the conjugation pad, dried at 25 °C for 2 h, and stored in a desiccator. The 6E3 antibody and goat anti-human IgG (1 mg/mL) were immobilized on the NC membrane as the test and control lines, respectively. After the NC membrane was dried, the membrane was blocked with 1% BSA. All components were assembled on the backing card, and the final LFA test strip was transferred to a strip cassette. For the assay, 150 μL of the sample was directly applied to the sample pad and spread across the strip within 5 min.

For the RT-PCR assay, the following primers were used according to previous literature (E. van der Vries et al., 2013); H275Y F: 5′ AAAAGGGGAAGGTTACTAAATCAATAGAGT, H275Y R: 5′ CAGTGTCTGGGTAACAGGAGCATT. A total of nine sets were tested, one set consisted of no template control (NTC), bare, WT pH1N1-spiked, and H275Y mutant pH1N1-spiked human nasopharyngeal aspirate samples. Viral RNA of each sample was extracted by using QIA amp viral RNA mini kit (Qiagen, VT, Australia) following standard protocol. Each RT-PCR reaction mixture contained 10 μL of *AccuPower greenstar* RT-qPCR 2 × master mix (Bioneer, Daejeon, Korea), 10 pmole of each primer, and 10 ng of RNA template in a final volume of 20 μL. Each reaction was performed using the following amplification conditions: reverse transcription reaction to get cDNA at 60 °C for 15 min, and PCR amplification at 95 °C for 3 min, followed by 40 cycles at 95 °C for 30 s and 62 °C for 30 s. Amplification and detection was performed on a CFX96 Touch RT-PCR detection system (Biorad, CA, USA) using the carboxy-X-rhodamine (ROX) filter (578–604 nm).

2.6. 6E3 antibody-mediated SERS immunoassay

For the preparation of the Au nanoplate immune substrate, Au nanoplates were synthesized in a vapor-phase as previously described (Yoo et al., 2017). As-synthesized Au nanoplates were incubated with Cys3-protein G solution in PBS (10 nM) for 18 h at 4 °C and rinsed with PBS three times. The protein G-modified Au nanoplates were incubated with 6E3 antibody in PBS (100 ng/mL) for 18 h at 4 °C and rinsed with PBS three times. For preparing the Au NP immunoprobes, 100 μL MGITC in ethanol (10 μM) was added to the Au NP solution to a final volume of

1 mL, and the Au NP solution was incubated for 45 min at 25 °C under orbital shaking. Next, the solution was centrifuged (13,500×g) for 15 min and resuspended in PBS. Next, 10 μL HS–$(CH_2)_{10}$–NHS in tetrahydrofuran (10 μM) and 100 μL 6E3 antibody in PBS (100 ng/mL), were mixed and the solution was stored for 45 min at 4 °C under orbital shaking. The mixed solution (50 μL) was added to the prepared Au NP solution, and this solution was incubated for 45 min at 25 °C under orbital shaking. Thereafter, 1.15 μL Tris-HCl buffer (1 M, pH 6.8) was added to the Au NP solution for 30 min at 25 °C under orbital shaking. Lastly, the Au NP solution was centrifuged (13,500×g) for 15 min and resuspended in PBS.

For the detection of viruses, various concentrations of the H275Y and WT viruses were diluted in PBS. The virus samples were incubated with immune substrates for 1 h at 4 °C under shaking. Then, the immune substrates were rinsed with PBS three times and incubated in the Au NP immunoprobe solution for 45 min at 25 °C. SERS spectra were measured after washing with distilled water and drying with N_2 gas. A micro-Raman system based on an Olympus BX41 microscope (Nanobase, Seongnam, Korea) was used for the SERS measurements. The excitation source was a He–Ne laser operating at λ = 633 nm (20 μW). The laser spot was focused on a sample through a 50 × objective lens. The SERS signals were recorded with a thermodynamically cooled electron-multiplying charge-coupled device mounted on a spectrometer with a 1200-groove/mm grating. SEM images were obtained on a Nova 230 system at an accelerating voltage of 15 keV (FEI, OR, USA).

Nasopharyngeal aspirate samples from patients were collected with the flocked nasopharyngeal swabs and transferred to the virus transport media (UTM, Copan Diagnostics Inc., CA, USA). All samples were stored at −70 °C before use. The protocol for this retrospective study was reviewed and approved by the Institutional Review Board of Yonsei University Health Service, Severance Hospital, Seoul, Korea (IRB approval number: 4-2017-1179). For the detection of viruses in human nasopharyngeal aspirate samples, the collected samples were thawed at 25 °C, and 10 μL influenza viruses (10^3 PFU/mL; WT or H275Y pH1N1) were spiked into each specimen (90 μL). The virus-spiked samples were diluted 10-fold with PBS and were used as the samples for diagnosis.

3. Results

3.1. Production of 6E3 antibody

For the development of a monoclonal antibody against the oseltamivir-resistant influenza virus, we employed a large human antigen-binding fragment (Fab) phage display library and a biopanning protocol including a subtraction step against WT NA. Fig. 1A shows the ELISA results for monoclonal phages after different rounds of panning. Upon further rounds of panning, WT NA binders were removed (red column in Fig. 1A), and H275Y NA-specific phages remained (blue column in Fig. 1A). After three rounds of biopanning, the clone that strongly bound the H275Y NA (6E3) was subjected to DNA sequencing, obtaining the unique clone shown in Fig. 1B. Finally, we converted the Fab form of 6E3 to the whole immunoglobulin G (IgG) form (6E3 antibody) for use in the diagnosis of H275Y-bearing antiviral drug-resistant influenza virus (Fig. 1C).

3.2. Binding of 6E3 antibody to H275Y NA

After the production of the 6E3 antibody, the binding affinities of the 6E3 antibody to WT and H275Y NA were measured by ELISA (Fig. 2A). The 6E3 antibody strongly bound to H275Y NA with a dissociation constant (K_D) of 32.76 pM. In contrast, the K_D of the 6E3 antibody to WT NA was 72.74 μM. The cross-reactivity of the 6E3 antibody was also examined by ELISA (Fig. 2B). The absorbance values increased only in the presence of H275Y NA. The absorbance values of bovine serum albumin (BSA), DENV1-EP, HG-NS1-3-6H, CHIKV-EP2, and JEV-E domain III were comparable to that of WT NA. These results indicate that the selected 6E3 antibody can specifically recognize the H275Y NA.

In Fig. 2C and D, the calculated binding modes of the 6E3 model epitopes in the WT and H275Y mutant NAs are displayed. The two epitopes appear to reveal a similar complexation pattern in the complementarity determining region (CDR) of 6E3. Most remarkably, the aromatic side chain of 275 residue points toward a small hydrophobic pocket comprising the three tryptophan residues of 6E3 (Trp 33
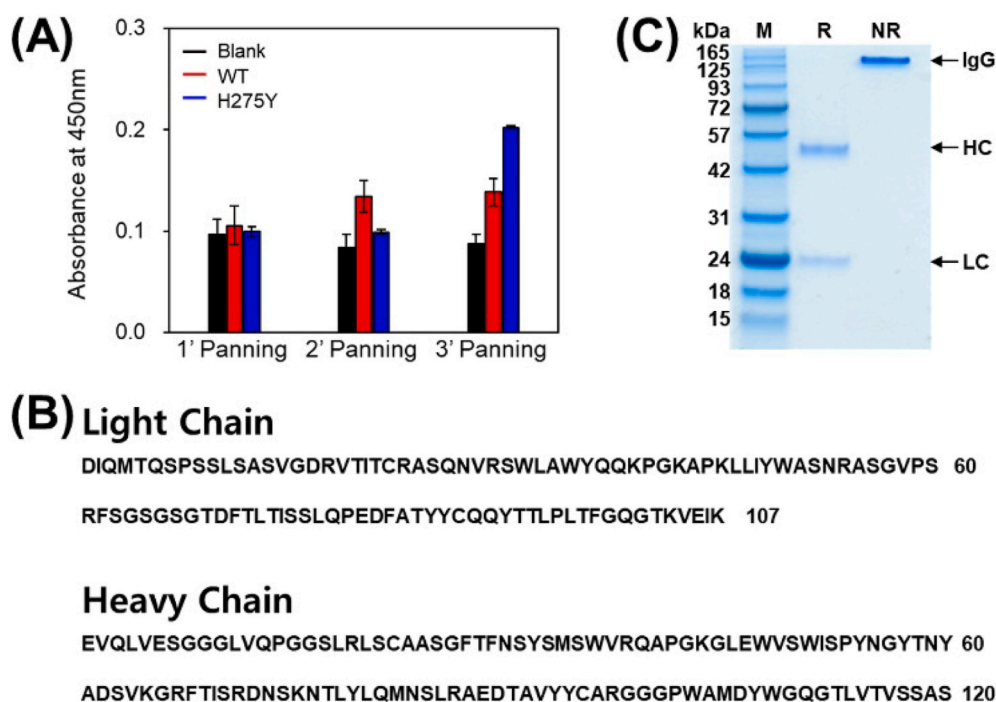

(B) Light Chain

DIQMTQSPSSLSASVGDRVTITCRASQNVRSWLAWYQQKPGKAPKLLIYWASNRASGVPS 60

RFSGSGSGTDFTLTISSLQPEDFATYYCQQYTTLPLTFGQGTKVEIK 107

Heavy Chain

EVQLVESGGGLVQPGGSLRLSCAASGFTFNSYSMSWVRQAPGKGLEWVSWISPYNGYTNY 60

ADSVKGRFTISRDNSKNTLYLQMNSLRAEDTAVYYCARGGGPWAMDYWGQGTLVTVSSAS 120

Fig. 1. (A) Screening for the H275Y NA specificity of the monoclonal phages from three rounds of panning by ELISA with HRP-conjugated αM13. Error bars = standard deviation (n = 3). (B) Amino acid sequence of 6E3. (C) SDS-PAGE analysis of purified 6E3 under reducing (R) and non-reducing (NR) conditions. Lane M: protein marker; HC: heavy chain; LC: light chain.
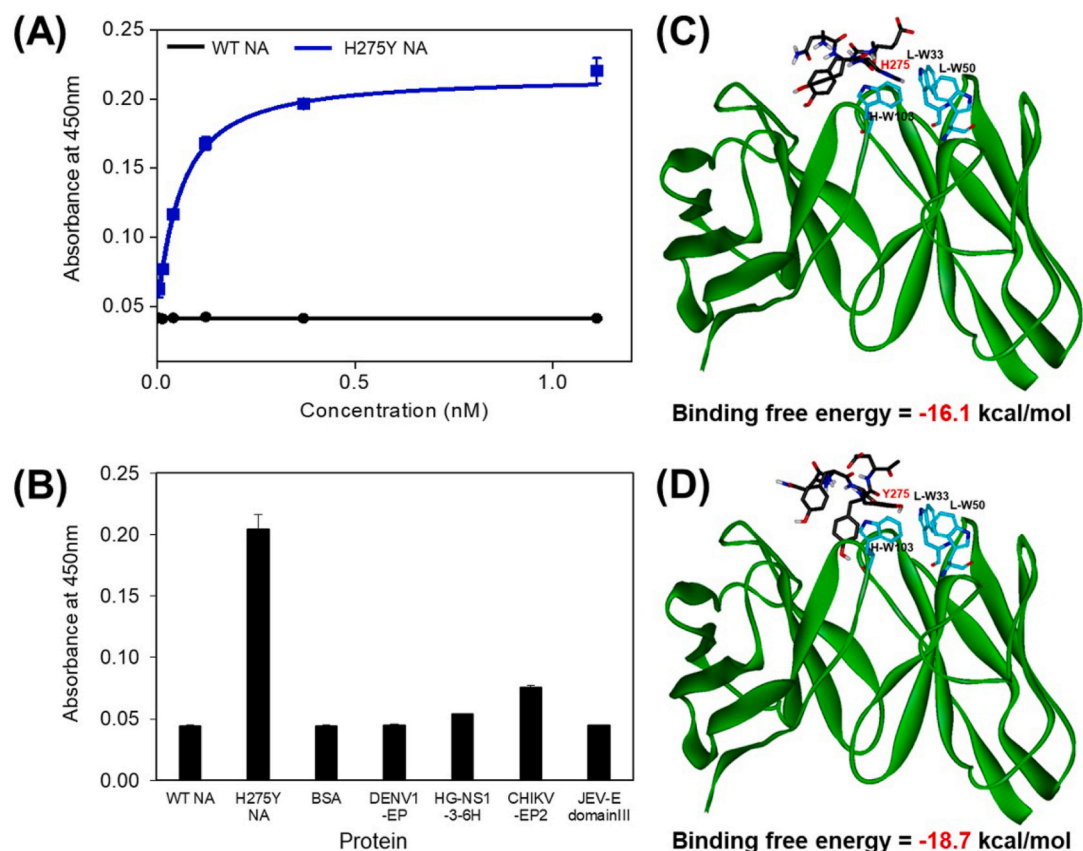
Fig. 2. (A) Plot of absorbance at 450 nm as a function of WT (black) and H275Y (blue) NA concentration. Error bars = standard deviation (n = 3). (B) Plot of absorbance at 450 nm *versus* proteins. Absorbance at 450 nm increased only in the presence of H275Y NA. Error bars = standard deviation (n = 3). (C, D) Docking conformation and calculated binding free energies of the model epitopes for (C) WT and (D) H275Y NAs in the CDR of 6E3 antibody. (For interpretation of the references to color in this figure legend, the reader is referred to the Web version of this article.)
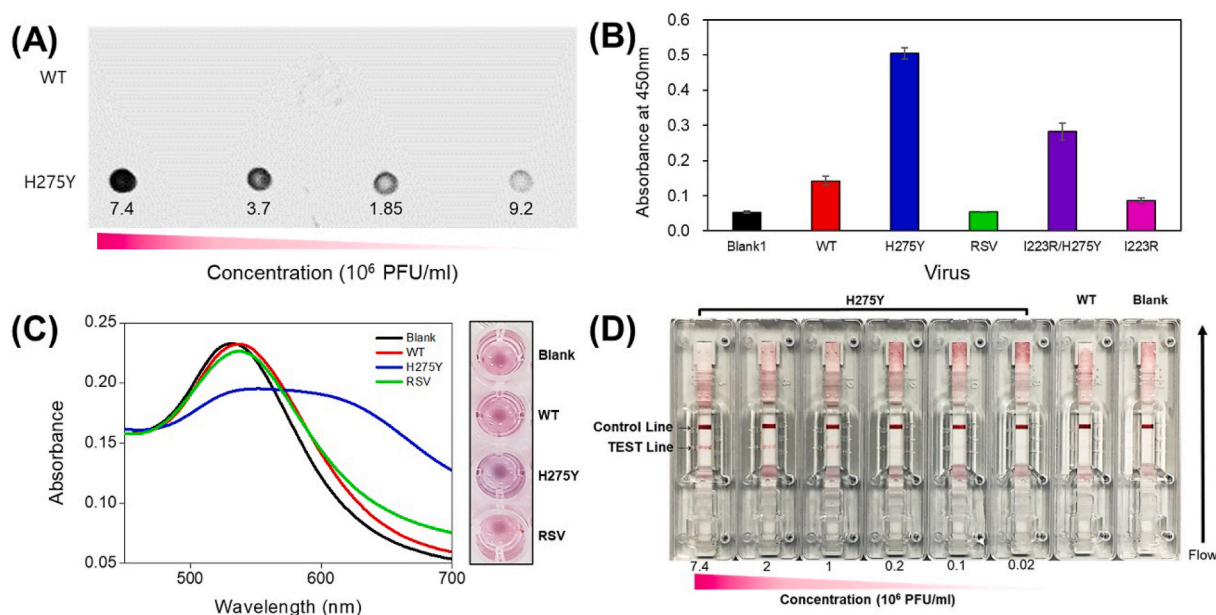

Fig. 3. (A) Specific interaction between the 6E3 antibody and H275Y pH1N1 virus by dot-blot analysis. The 6E3 antibody was applied to WT and H275Y pH1N1 viruses dotted in a two-fold dilution series from 0.92 to 7.4×10^6 PFU/mL. (B) The plot of absorbance at 450 nm *versus* viruses tested. Absorbance increased in the presence of H275Y or I223 R/H275Y mutant viruses. Error bars = standard deviation (n = 3). (C) Absorbance spectra (left) and photograph (right) of 6E3-Au NPs in the presence of blank, WT, and H275Y pH1N1 viruses and RSV samples. The concentration of each virus was 10^5 PFU/mL. (D) Photograph of lateral flow systems after the detection of H275Y pH1N1 virus ($0.02–7.4 \times 10^6$ PFU/mL), WT pH1N1 virus (7.4×10^6 PFU/mL), and blank samples.

and Trp 50 in the light chain, and Trp 103 in the heavy chain). The phenol side chain of Tyr275 in the mutant NA is closer than the imidazole group of His 275 in the WT NA to the tryptophan triad in 6E3. The van der Waals volume increases due to the substitution of tyrosine for histidine. As a consequence, the AutoDock binding free energy for the 6E3 antibody decreases from −16.1 to −18.7 kcal/mol as the epitope changes from the WT to H275Y mutant, which is consistent with the higher binding affinity to the latter. We further performed docking simulations using the extended 3-dimensional (3D) grid maps including the entire antibody structure, to check for the presence of the other stable binding configurations. No peripheral binding pocket in which an epitope could be complexed with the negative value of binding free energy was found. This supports the reliability of the docking poses derived from AutoDock.

3.3. Application of 6E3 antibody to H275Y pH1N1 detection

6E3 antibody was employed for the detection of oseltamivir-resistant pH1N1 by combining several techniques. First, dot-blot tests were accomplished using WT and H275Y mutant pH1N1 virus-spotted nitrocellulose (NC) membranes (Fig. 3A). On the mutant pH1N1-spotted membrane, distinct spots were observed in a virus-concentration dependent manner. On the WT virus-spotted membrane, no spots were observed. The dot-blot tests clearly show that the 6E3 antibody can detect the H275Y mutant influenza virus.

Second, ELISA tests were performed using WT, H275Y, I223R, I223R/H275Y mutant viruses and human respiratory syncytial virus A2 (RSV). Absorbance significantly increased in the presence of the H275Y mutant virus (Fig. 3B). In the presence of WT, I223R pH1N1, and RSV, weak signals were obtained (Fig. 3B). Interestingly, the 6E3 antibody could recognize the double-mutant virus (I223 R/H275Y pH1N1) (purple bar in Fig. 3B). Previous study revealed that the H275Y substitution has a major effect on the binding pose within the active site while the influence of other mutations is much less prominent (Pokorná et al., 2018). This might attribute that the 6E3 antibody recognizes not only the H275Y mutation but also I223 R/H275Y double mutations.

Third, the 6E3 antibody was combined with Au NPs for colorimetric detection of the H275Y mutant virus. The bare 6E3-Au NPs exhibit reddish color with maximum absorption at 534 nm (black spectrum in Fig. 3C). When the 6E3-Au NPs were mixed with WT pH1N1 or RSV, the color and absorbance of the NPs were preserved (Fig. 3C). When the 6E3-NPs were mixed with the oseltamivir-resistant virus, the absorbance peak was red-shifted and broadened (Fig. 3C). The color of 6E3-NPs also changed to purple after mixing with H275Y pH1N1. This change is attributed to the binding of the 6E3-NP to the H275Y NA of mutant viruses.

Lastly, LFA for the H275Y pH1N1 virus was developed using the 6E3 antibody. Briefly, the anti-influenza A nucleoprotein IgG-Au NPs were added to the conjugation pad as a detection probe. The 6E3 antibody and the goat anti-human IgG were lined on the NC membrane as the test and control lines, respectively. This LFA test strip is expected to display two red lines (test and control lines) when the H275Y mutant pH1N1 virus is present in a sample. As shown in Fig. 3D, the test lines showed reddish colors after the addition of the H275Y mutant viruses to the membranes. The color of the test line became more distinct with increasing concentrations of the mutant virus. By using the developed LFA test strip, the H275Y pH1N1 virus could be detected at a low concentration of 2×10^5 plaque-forming units (PFU)/mL. At a lower concentration, the red line was indistinguishable. The LFA did not react with the WT pH1N1 (7.4×10^6 PFU/mL). The blank sample also showed no signal.

3.4. 6E3 antibody-mediated SERS immunoassay for H275Y pH1N1

Although the 6E3 antibody was applied to several kinds of approaches for the detection of the H275Y mutant virus, the detection limits were still high and needed improvement. Therefore, we tried to

combine the 6E3 antibody with the SERS-based immunoassay using atomically flat Au nanoplates. The well-immobilized bioreceptors on flat and clean surfaces are promising immune substrates in the development of high-performance immunological sensors as they can provide reproducible SERS signals and prevent nonspecific binding (Hwang et al., 2019). Previous reports support that the atomically flat Au nanoplate platforms enable the sensitive and selective detection of biomolecules (Eom et al., 2019a,b; Hwang et al., 2019; Lee et al., 2018). The schematic illustration of the H275Y mutant virus detection by 6E3 antibody-mediated SERS immunoassay is shown in Fig. 4A. For the preparation of the immune substrate, the 6E3 antibody was immobilized on a single-crystalline Au nanoplate. In brief, the vapor-phase grown Au nanoplates were incubated with three cysteine-tagged protein G (Cys3-protein G) and washed. Protein G binds the crystallizable fragment (Fc) of an antibody, thereby enabling effective exposure of the antibody to its antigen (Hwang et al., 2019). Next, the 6E3 antibody was immobilized on the protein G-coated Au nanoplate and washed. For the preparation of the immunoprobes, the surfaces of Au NPs were simultaneously modified with 6E3 antibody and MGITC, a well-known Raman reporter (Sharma et al., 2012). In this experiment, we immobilized the 6E3 antibody on both Au nanoplates and NPs to increase the specificity of the H275Y pH1N1 virus detection. In general sandwich immunoassays, two different types of antibodies are employed (Deiss et al., 2009; Rissin and Walt, 2006; Sánchez-Purrà et al., 2017). The current SERS-based immunoassay, however, employed a single 6E3 antibody because a single pH1N1 virus particle has over 200 NA proteins (Eom et al., 2019a,b), allowing a sufficient 6E3-H275Y-6E3 sandwich formation. For the detection of the drug-resistant virus using the 6E3-mediated SERS immunoassay, the 6E3-Au nanoplates were allowed to react with virus samples (WT or H275Y pH1N1), and the immunoprobes were incubated. In the presence of the H275Y mutant virus, the Au NP-on-nanoplate structure can be formed. This nanostructure can provide strong SERS signals of MGITC near the gaps between the NPs and the nanoplate. In contrast, in the presence of only the WT pH1N1 virus, the Au NPs do not assemble on the nanoplate, yielding negligible SERS signals.

We then examined the results of H275Y pH1N1 virus detection using the 6E3 antibody-mediated SERS immunoassay. As shown in Fig. 4B, the control sample showed no SERS signal. Meanwhile, the SERS signals of MGITC increased with increasing mutant virus concentrations. The scanning electron microscope (SEM) images of Au NPs-on-nanoplate structures from which we obtained the SERS signals are shown in Fig. S1 of Supporting Information. The SERS signals for 10^2 PFU/mL of the mutant pH1N1 are distinguishable from those of the control sample, indicating that the detection limit of the 6E3 antibody-mediated SERS immunoassay is 10^2 PFU/mL. Fig. 4C is the plot of integrated 1615 cm^{-1} band intensity as functions of WT and H275Y pH1N1 virus concentrations. This further suggests that the 6E3 antibody-mediated SERS immunoassay can detect the mutant virus quantitatively. In addition, we investigated the selective detection of the H275Y mutant virus in a mixture of WT and mutant viruses using the SERS-based method. In the mixture samples, the number of H275Y pH1N1 mutant viruses was varied at 0, 10^2, 10^3, 10^4 and 10^5 PFU/mL and the number of WT pH1N1 viruses was fixed at 10^5 PFU/mL. As shown in Fig. S2, the SERS signals of MGITC gradually increased as the concentration of H275Y mutant virus increased. The 6E3 antibody-mediated SERS immunoassay could detect 0.1% H275Y mutant virus in the mutant (10^2 PFU/mL) and WT (10^5 PFU/mL) virus-coexisting mixture. Notably, the SERS signals for WT pH1N1 detection are negligible regardless of virus concentration. Thus, the 6E3 antibody and Au nanoplate platform synergistically contributed to the sensitive and selective detection of the oseltamivir-resistant influenza virus.
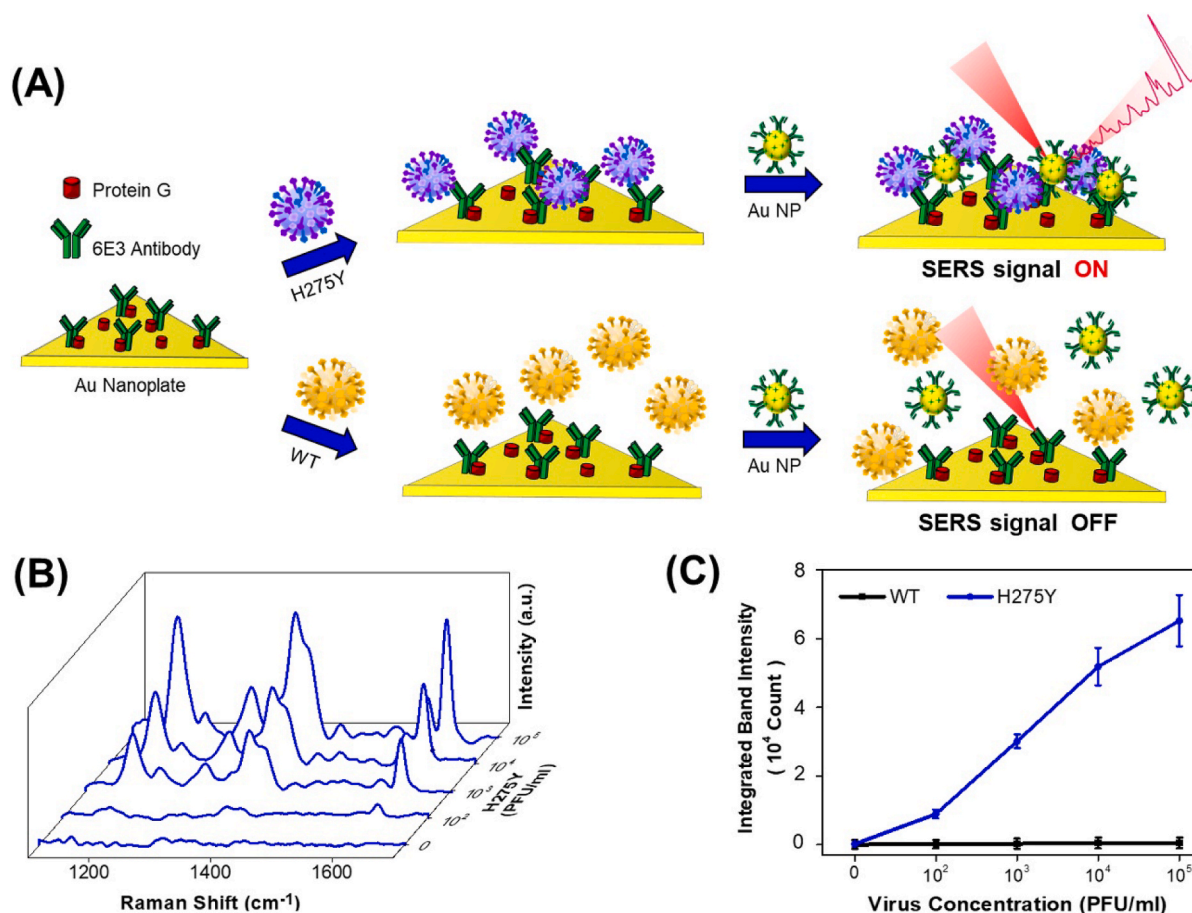
Fig. 4. (A) Schematic illustration of 6E3 antibody-mediated SERS immunoassay for WT and H275Y pH1N1 viruses. (B) SERS spectra of MGITC as a function of H275Y pH1N1 concentration (0, 10^2, 10^3, 10^4, and 10^5 PFU/mL). (C) Plot of integrated 1615 cm^{-1} band intensity *versus* WT pH1N1 and H275Y pH1N1 virus concentrations. Error bars = standard deviation (n = 10).

3.5. Direct detection of H275Y pH1N1 in human nasopharyngeal aspirate

The human nasopharyngeal aspirate samples are most frequently used for the diagnosis of respiratory virus infection in patients (Paton et al., 1992; Peiris et al., 2003). Therefore, we tried to detect the oseltamivir-resistant virus in the human nasopharyngeal aspirate using the 6E3 antibody-mediated SERS immunoassay. The nasopharyngeal samples were provided from a tertiary hospital in Korea after approval. These samples were collected from the patients with flu symptoms but who were negatively diagnosed for flu. As the presence of antiviral drug-resistant viruses is currently not tested in the hospital, the H275Y mutant virus was intentionally added into the collected nasopharyngeal swab samples and examined by the 6E3 antibody-mediated SERS immunoassay (Fig. 5A). A total of nine H275Y pH1N1-spiked human nasopharyngeal aspirate samples was examined, and the final concentration of the H275Y virus was 10^3 PFU/mL. Fig. 5B shows the SERS spectra of MGITC after the detection of the H275Y mutant virus in human nasopharyngeal aspirate samples using the 6E3-mediated SERS immunoassay. All nine samples provided positive SERS signals, indicating the successful detection of the mutant viruses. Note that the H275Y pH1N1-spiked nasopharyngeal swab samples were directly employed without pre-treatment steps. This suggests that the assay is useful for the diagnosis of drug-resistant pH1N1 virus-infected patients. We further investigated the 6E3-mediated SERS immunoassay by comparing the diagnostic results of H275Y pH1N1- and WT pH1N1-spiked nasopharyngeal aspirate and control samples. Blue bars in Fig. 5C represent the integrated 1615 cm^{-1} band intensities obtained

from the mutant virus-spiked human nasopharyngeal aspirates samples, corresponding to the result of Fig. 5B. Red bars are the integrated band intensities from the WT pH1N1-spiked samples. Black bars are the integrated band intensities from the bare nasal samples. The full SERS spectra of Fig. 5C are shown in Fig. S2 of Supporting Information. Strong SERS signals were observed only in the presence of H275Y pH1N1, indicating that 6E3 antibody-mediated SERS immunoassay can recognize the mutant virus in human nasopharyngeal aspirate samples. The fluctuating SERS signals in the control and WT pH1N1-spiked nasopharyngeal aspirate samples may be attributed to nonspecific binding with biological species in the nasopharyngeal aspirate samples. Nevertheless, all H275Y-spiked nasopharyngeal aspirate samples provided positive SERS signals, proving accurate diagnosis of the oseltamivir-resistant pH1N1. The PCR result also agrees well with the SERS result (Fig. S4).

4. Discussion

Influenza viruses cause seasonal epidemics almost every winter. Patients with flu symptoms such as coughs, sore throat, fever, etc., are diagnosed in hospitals through RIDTs. When the test result is positive for influenza viruses, a doctor may prescribe an antiviral medication such as oseltamivir, zanamivir, etc. Unfortunately, drug-resistant influenza viruses are becoming increasingly dominant; a previous report suggested that 27% of A H1N1 virus-infected children exhibited resistance after treatment with oseltamivir (Stephenson et al., 2009). Thus, the growing number of drug-resistant pH1N1 viruses is a cause of concern for the treatment of flu patients. To address this issue, the Centers for Disease
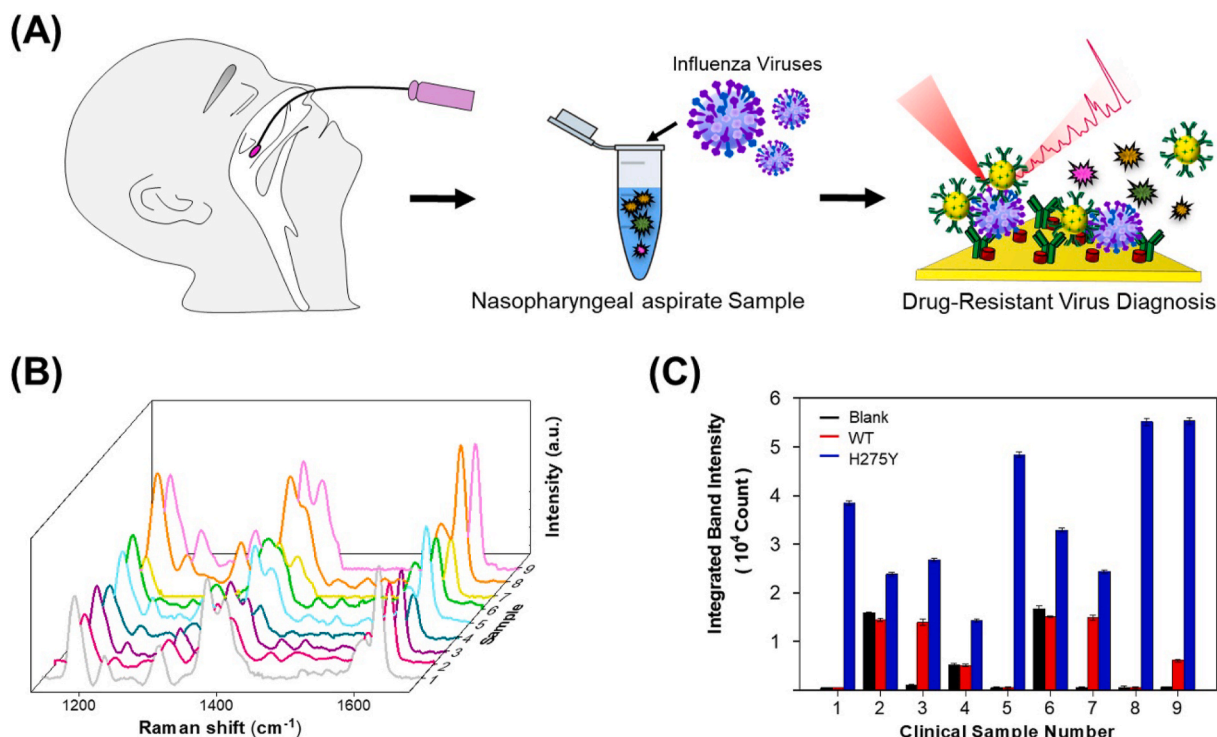
Fig. 5. (A) Schematic illustration of drug-resistant virus detection in human nasopharyngeal aspirate sample. (B) SERS spectra of MGITC as a function of H275Y pH1N1-spiked human nasopharyngeal aspirate samples. (C) Plot of integrated 1615 cm^{-1} band intensity *versus* WT pH1N1-spiked, H275Y pH1N1-spiked, and bare human nasopharyngeal aspirate samples. Error bars = standard deviation (n = 10).

Control and Prevention of the United States (CDC) conducts ongoing surveillance and testing for seasonal and novel influenza viruses with reduced susceptibility and acquired resistance to antivirals (Oko-mo-Adhiambo et al., 2014). NA inhibitors (NAIs), that selectively target the NA of pH1N1, play a key role in the management of influenza infection (Hussain et al., 2017; Lackenby et al., 2018; Ishiguro et al., 2018). Because NAIs remain the only widely licensed class of antiviral drugs appropriate for the treatment and prophylaxis of seasonal flu (Ishiguro et al., 2018; Earn et al., 2002). Given the very limited number of anti-influenza therapeutic agents, preparedness for a potential future influenza pandemic has focused on the emergence of NAI-resistant virus mutations (Ishiguro et al., 2018; Earn et al., 2002; Baranovich et al., 2010). Among the limited NAIs, oseltamivir has been most extensively prescribed (Ishiguro et al., 2018; Laplante et al., 2014). Therefore, the NA mutations exhibiting the oseltamivir resistance have been most frequently reported (Laplante et al., 2014). Considering that numerous research results of drug resistance are related to H275Y mutation (Laplante et al., 2014; Kelso and Hurt, 2012; Pizzorno et al., 2011), it is urgently required to develop the identification methods for H275Y NA mutation.

Previously, we developed oseltamivir hexylthiol (OHT) as a chemical receptor for the H275Y pH1N1 virus (Eom et al., 2019a,b; Hwang et al., 2018). The A4 antibody against the double-mutant influenza viruses was also developed by our group (Guk et al., 2020). In this study, we report a 6E3 antibody against the H275Y mutant pH1N1 influenza virus. The strong binding affinity of the 6E3 antibody to H275Y NA enables the recognition of the oseltamivir-resistant pH1N1 virus. Compared with a chemical receptor, an antibody could be used for a wider range of immunoassays. Moreover, the 6E3 antibody could have a higher value than the A4 antibody in clinical diagnostic uses as the 6E3 antibody recognizes not only H275Y mutation but also I223 R/H275Y double mutations. In fact, the H275Y mutation occurs much more frequently than the I223 R/H275Y double mutations (Paradis et al., 2015). Furthermore, we developed an advanced immunological approach for detecting drug-resistant viruses in human nasopharyngeal aspirate samples by

combining the 6E3 antibody with nanomaterials. The previous SERS approach using the A4 antibody simply demonstrated the detection of the double mutant virus in the buffer (Guk et al., 2020). More importantly, we shortened the detection time of SERS immunoassay from 7 to 2 h in this study. Recently, immunoassays have been combined with various nanotechnologies for developing sophisticated and sensitive sensing methods (Lee et al., 2018). The SERS immunoassay developed in this study for detecting drug-resistant pH1N1 influenza viruses may contribute to the prevention of severe diseases by ensuring appropriate treatments. As two kinds of biological (6E3 antibody) and chemical (OHT) receptors are available for the detection of the oseltamivir-resistant virus, in the future, we will try to fuse these two molecules and apply them to high-quality nanomaterials to further increase the precision of diagnosis of the drug-resistant pH1N1 influenza virus.

5. Conclusion

In this study, we developed the 6E3 antibody against the H275Y mutant pH1N1 influenza virus with a K_D of 32.76 pM for H275Y NA. The 6E3 antibody was applied to dot-blot, ELISA, colorimetry, and LFA, showing wide applicability. We also immobilized the 6E3 antibody to an Au nanoplate and NPs to demonstrate SERS-based detection of the H275Y mutant pH1N1 virus. The 6E3-mediated SERS immunoassay allowed the detection of the drug-resistant virus at a low concentration of 10^2 PFU/mL. We also verified that the developed assay could be useful for the diagnosis of H275Y pH1N1 in human nasopharyngeal aspirate samples. The present results provide a new method for diagnosing antiviral drug-resistant influenza viruses and further contribute to the prevention of the re-emergence of infectious diseases.

Declaration of competing interest

The authors declare that they have no known competing financial interests or personal relationships that could have appeared to influence

the work reported in this paper.

Acknowledgments

Appendix A. Supplementary data

Supplementary data to this article can be found online at https://doi.org/10.1016/j.bios.2021.113324.

Author contribution

Hyeran Kim: Validation, Formal analysis, Investigation, Resources, Data curation, Writing – review & editing, Visualization, Hyunju Kang: Methodology, Validation, Formal analysis, Investigation, Data curation, Writing – original draft, Writing – review & editing, Visualization, Hye-Nan Kim: Investigation, Hongki Kim: Investigation, Jeong Moon: Investigation, Kyeonghye Guk: Investigation, Hwangseo Park: Software, Resources, Data curation, Visualization, Dongeun Yong: Resources, Pan Kee Bae: Resources, Hyun Gyu Park: Project administration, Eun-Kyung Lim: Project administration, Taejoon Kang: Conceptualization, Methodology, Data curation, Writing – original draft, Writing – review & editing, Visualization, Supervision, Project administration, Funding acquisition, Juyeon Jung: Conceptualization, Methodology, Data curation, Writing – original draft, Writing – review & editing, Supervision, Project administration, Funding acquisition

Data availability

The datasets used and/or analyzed during the current study are available from the corresponding author upon reasonable request.

References

Kelso, A., Hurt, A.C., 2012. Nat. Med 18, 1470–1471.
Baranovich, T., Saito, R., Suzuki, Y., Zaraket, H., Dapat, C., Caperig-Dapat, I., Oguma, T., Shabana, I.I., Saito, T., Suzuki, H., 2010. J. Clin. Virol. 47, 23–28.
Bedford, T., Riley, S., Barr, I.G., Broor, S., Chadha, M., Cox, N.J., Daniels, R.S., Gunasekaran, C.P., Hurt, A.C., Kelso, A., 2015. Nature 523, 217–220.
Brookes, D.W., Miah, S., Lackenby, A., Hartgroves, L., Barclay, W.S., 2011. Antimicrob. Chemother 66, 466–470.
Deiss, F., LaFratta, C.N., Symer, M., Blicharz, T.M., Sojic, N., Walt, D.R., 2009. J. Am. Chem. Soc. 131, 6088–6089.
Earn, D.J., Dushoff, J., Levin, S.A., 2002. Trends ecol. Evolution 17, 334–340.
Eom, G., Hwang, A., Lee, D.K., Guk, K., Moon, J., Jeong, J., Jung, J., Kim, B., Lim, E.-K., Kang, T., 2019a. ACS appl. Bio Mater 2, 1233–1240.
Eom, G., Hwang, A., Kim, H., Yang, S., Lee, D.K., Song, S., Ha, K., Jeong, J., Jung, J., Lim, E.-K., 2019b. ACS Sens. 4, 2282–2287.
Fiser, A., Do, R.K.G., Šali, A., 2000. Protein Sci. 9, 1753–1773.
Ginting, T.E., Shinya, K., Kyan, Y., Makino, A., Matsumoto, N., Kaneda, S., Kawaoka, Y., 2012. J. Virol. 86, 121–127.
Green, D.A., StGeorge, K., 2018. J. Clin. Microbiol. 56, e00711–e00718.
Guk, K., Kim, H., Lee, M., Choi, Y.-A., Hwang, S.G., Han, G., Kim, H.-N., Kim, H., Park, H., Yong, D., Kang, T., Lim, E.K., Jung, J., 2020. Nat. Commun. Now. 11, 1–11.
Hayden, F.G., de Jong, M.D., 2011. J. Infect. Dis. 203, 6–10.
Hayden, F.G., Osterhaus, A.D., Treanor, J.J., Fleming, D.M., Aoki, F.Y., Nicholson, K.G., Bohnen, A.M., Hirst, H.M., Keene, O., Wightman, K., 1997. New engl. J. Med. 337, 874–880.
Hurt, A.C., 2014. Curr. Opin. Virol 8, 22–29.
Hussain, M., Galvin, H.D., Haw, T.Y., Nutsford, A.N., Husain, M., 2017. Infect. Drug Res. 10, 121–134.
Hwang, S.G., Ha, K., Guk, K., Lee, D.K., Eom, G., Song, S., Kang, T., Park, H., Jung, J., Lim, E.K., 2018. Sci. Rep. 8, 1–11.
Hwang, A., Kim, E., Moon, J., Lee, H., Lee, M., Jeong, J., Lim, E.-K., Jung, J., Kang, T., Kim, B., 2019. ACS appl. Mater. Interfaces 11, 18960–18967.
Ishiguro, N., Koseki, N., Kaiho, M., Ariga, T., Kikuta, H., Oba, K., Togashi, T., Morita, K., Inagawa, A., Okamura, A., 2018. J. Infect. Chemother. 24, 449–457.
Jang, W.S., Lim, D.H., Nam, J., Mihn, D.-C., Sung, H.W., Lim, C.S., Kim, J., 2020. PLoS One 15, e0238615.
Jones, S., Nelson-Sathi, S., Wang, Y., Prasad, R., Rayen, S., Nandel, V., Hu, Y., Zhang, W., Nair, R., Dharmaseelan, S., Chirundodh, D.V., Kumar, R., Pillai, R.M., 2019. Sci. Rep. 9, 1–10.
Kim, S., Park, I., Park, S.G., Cho, S., Kim, J.H., Ipper, N.S., Choi, S.S., Lee, E.S., Hong, H. J., 2017. Mol. Cell 40, 655–666.
Lackenby, A., Besselaar, T.G., Daniels, R.S., Fry, A., Gregory, V., Gubareva, L.V., Huang, W., Hurt, A.C., Leang, S.-K., Lee, R.T., 2018. Antivir. Res. 157, 38–46.
Laplante, J., George, K.S., 2014. Clin. Lab. Med. 34, 387–408.
Lee, M., Kim, H., Kim, E., Yi, S.Y., Hwang, S.G., Yang, S., Lim, E.-K., Kim, B., Jung, J., Kang, T., 2018. ACS appl. Mater. Interfaces 10, 37829–37834.
Marks, J.D., Hoogenboom, H.R., Bonnert, T.P., McCafferty, J., Griffiths, A.D., Winter, G., 1991. J. Mol. Biol. 222, 581–597.
McKimm-Breschkin, J.L., 2013. Influenza other respir. Viruses 7, 25–36.
Medina, R.A., García-Sastre, A., 2011. Nat. Rev. Microbiol. 9, 590–603.
Meijer, A., Lackenby, A., Hungnes, O., Lina, B., van der Werf, S., Schweiger, B., Opp, M., Paget, J., van de Kassteele, J., Hay, A., Emerg, M.Z., 2009. Infect. Dis 15, 552–560.
Morris, G.M., Goodsell, D.S., Halliday, R.S., Huey, R., Hart, W.E., Belew, R.K., Olson, A. J., 1998. J. Comput. Chem. 19, 1639–1662.
Moscona, A., 2005. New engl. J. Med. 353, 1363–1373.
Okomo-Adhiambo, M., Nguyen, H.T., Abd Elal, A., Sleeman, K., Fry, A.M., Gubareva, L. V., 2014. Influenza other respir. Viruses 8, 258–265.
Paradis, E.G., Pinilla, L.T., Holder, B.P., Abed, Y., Boivin, G., Beauchemin, C.A., 2015. PLoS One 10, e0126115.
Paton, A.W., Paton, J.C., Lawrence, A.J., Goldwater, P.N., Harris, R.J., 1992. J. Clin. Microbiol. 30, 901–904.
Peiris, J., Lai, S., Poon, L., Guan, Y., Yam, L., Lim, W., Nicholls, J., Yee, W., Yan, W., Cheung, M., Cheng, C., Chan, K., Tsang, D., Yung, R., Ng, T., Yuen, K., 2003. Lancet 361, 1319–1325.
Petrova, V.N., Russell, C.A., 2018. Nat. Rev. Microbiol. 16, 47–60.
Pizzorno, A., Abed, Y., Boivin, G., 2011. Influenza drug resistance, Seminars in respiratory and critical care medicine. © Thieme Medical Publishers, pp. 409–422.
Pokorná, J., Pachl, P., Karlukova, E., Hejdánek, J., Řezáčová, P., Machara, A., Hudlický, J., Konvalinka, J., Kožíšek, M., 2018. Viruses 10, 339.
Reid, A.H., Taubenberger, J.K., Fanning, T.G., 2004. Nat. Rev. Microbiol. 2, 909–914.
Rissin, D.M., Walt, D.R., 2006. Anal. Chim. Acta 564, 34–39.
Šali, A., Blundell, T.L., 1993. J. Mol. Biol. 234, 779–815.
Sánchez-Purrà, M., Carré-Camps, M., de Puig, H., Bosch, I., Gehrke, L., Hamad-Schifferli, K., 2017. ACS infect. Dis 3, 767–776.
Sharma, B., Frontiera, R.R., Henry, A.-I., Ringe, E., Van Duyne, R.P., 2012. Mater. Today Off. 15, 16–25.
Sharma, A., Tiwari, S., Deb, M.K., Marty, J.L., 2020. Antimicrob. Age 56, 106054.
Shetty, A.K., Peek, L.A., 2012. Expert rev. Anti-Infect. Ther 10, 123–143.
Stephenson, I., Democratis, J., Lackenby, A., McNally, T., Smith, J., Pareek, M., Ellis, J., Bermingham, A., Nicholson, K., Zambon, M., 2009. Clin. Infect. Dis. 48, 389–396.
Taubenberger, J.K., Kash, J.C., Morens, D.M., 2019. Sci. Transl. Med. 11, eaau5485.
Tolentino-Lopez, L., Segura-Cabrera, A., Reyes-Loyola, P., Zimic, M., Quiliano, M., Briz, V., Muñoz-Fernández, A., Rodríguez-Pérez, M., Ilizaliturri-Flores, I., Correa-Basurto, J., 2013. Biopolymers 99, 10–21.
Trombetta, V.K., Chan, Y.L., Bankowski, M.J., 2018. Hawai'i J. Med. Public Health 77 (9), 226–230.
Vijaykrishna, D., Poon, L., Zhu, H., Ma, S., Li, O., Cheung, C., Smith, G., Peiris, J., Guan, Y., 2010. Science 328, 1529–1529.
van der Vries, E., Anber, J., van der Linden, A., Wu, Y., Maaskant, J., Stadhouders, R., van Beek, R., Rimmelzwaan, G., Osterhaus, A., Boucher, C., 2013. J. Mol. Diagn. 15, 347–354.
Yoo, Y., Lee, H., Lee, H., Lee, M., Yang, S., Hwang, A., Kim, S.-I., Park, J.Y., Choo, J., Kang, T., Kim, B., 2017. Chem. Mater. 29, 8747–8756.
Yoon, S.O., Lee, T.S., Kim, S.J., Jang, M.H., Kang, Y.J., Park, J.H., Kim, K.-S., Lee, H.S., Ryu, C.J., Gonzales, N.R., Kashmiri, S.V.S., Lim, S.M., Choi, C.W., Hong, H.J., 2006. J. Biol. Chem. 281, 6985–6992.
Yu, C.M., Peng, H.P., Chen, C., Lee, Y.C., Chen, J.B., Tsai, K.C., Chen, C.T., Chang, J.Y., Yang, E.W., Hsu, P.C., Jian, J.W., Hsu, H.J., Chang, H.J., Hsu, W.L., Huang, K.F., Ma, A.C., Yang, A.S., 2012. PloS One 7, e33340.